



## **Ba<sub>1-x</sub>Sr<sub>x</sub>TiO<sub>3</sub> Based Thin Films for Next Generation Devices**

**Eric Ngo, William D. Nothwang, Clifford Hubbard, Samuel Hirsch,  
Melanie W. Cole, Wontae Chang, Steven W. Kirchoffer, and Jeff M. Pond**

**ARL-TN-228**

**September 2004**

## **NOTICES**

### **Disclaimers**

The findings in this report are not to be construed as an official Department of the Army position unless so designated by other authorized documents.

Citation of manufacturer's or trade names does not constitute an official endorsement or approval of the use thereof.

Destroy this report when it is no longer needed. Do not return it to the originator.

# **Army Research Laboratory**

Aberdeen Proving Ground, MD 21005-5069

---

---

**ARL-TN-228**

**September 2004**

---

## **Ba<sub>1-x</sub>Sr<sub>x</sub>TiO<sub>3</sub> Based Thin Films for Next Generation Devices**

**Eric Ngo, William D. Nothwang, Clifford Hubbard, Samuel Hirsch,  
and Melanie W. Cole**

**Weapons and Materials Research Directorate, ARL**

**Wontae Chang, Steven W. Kirchoffer, and Jeff M. Pond**

**U.S. Naval Research Laboratory,  
Washington, DC**

REPORT DOCUMENTATION PAGE			Form Approved OMB No. 0704-0188		
Public reporting burden for this collection of information is estimated to average 1 hour per response, including the time for reviewing instructions, searching existing data sources, gathering and maintaining the data needed, and completing and reviewing the collection information. Send comments regarding this burden estimate or any other aspect of this collection of information, including suggestions for reducing the burden, to Department of Defense, Washington Headquarters Services, Directorate for Information Operations and Reports (0704-0188), 1215 Jefferson Davis Highway, Suite 1204, Arlington, VA 22202-4302. Respondents should be aware that notwithstanding any other provision of law, no person shall be subject to any penalty for failing to comply with a collection of information if it does not display a currently valid OMB control number. <b>PLEASE DO NOT RETURN YOUR FORM TO THE ABOVE ADDRESS.</b>					
1. REPORT DATE (DD-MM-YYYY) September 2004		2. REPORT TYPE Final		3. DATES COVERED (From - To) November 2003–April 2004	
4. TITLE AND SUBTITLE Ba <sub>1-x</sub> Sr <sub>x</sub> TiO <sub>3</sub> Based Thin Films for Next Generation Devices			5a. CONTRACT NUMBER		
			5b. GRANT NUMBER		
			5c. PROGRAM ELEMENT NUMBER		
6. AUTHOR(S) Eric Ngo, William D. Nothwang, Clifford Hubbard, Samuel Hirsch, Melanie W. Cole, Wontae Chang,* Steven W. Kirchoffer,* and Jeff M. Pond*			5d. PROJECT NUMBER AH84		
			5e. TASK NUMBER		
			5f. WORK UNIT NUMBER		
7. PERFORMING ORGANIZATION NAME(S) AND ADDRESS(ES) U.S. Army Research Laboratory ATTN: AMSRD-ARL-WM-MA Aberdeen Proving Ground, MD 21005-5069			8. PERFORMING ORGANIZATION REPORT NUMBER ARL-TN-228		
9. SPONSORING/MONITORING AGENCY NAME(S) AND ADDRESS(ES)			10. SPONSOR/MONITOR'S ACRONYM(S)		
			11. SPONSOR/MONITOR'S REPORT NUMBER(S)		
12. DISTRIBUTION/AVAILABILITY STATEMENT Approved for public release; distribution is unlimited.					
13. SUPPLEMENTARY NOTES *U.S. Naval Research Laboratory, Microwave Division, 4550 Overlook Ave. SW, Washington, DC 20375					
14. ABSTRACT Over the past several years, there has been a tremendous growth and development of thin film deposition technology in the electronics industry. Ferroelectric thin films have been recognized for their unique dielectric properties and appear to be desirable for tunable microwave device applications. Among the most promising candidates for such applications are Ba <sub>1-x</sub> Sr <sub>x</sub> TiO <sub>3</sub> (BST) and BST-based thin films. In this work, pure BST and acceptor doped BST-based thin films were fabricated on (100) MgO substrates via pulsed laser deposition. X-ray diffraction, in conjunction with the atomic force microscope, was used to analyze the film crystallinity and surface morphology. The dielectric properties were characterized at both 100 kHz and 20 GHz. The metal-insulator-metal capacitor configuration was used to attain the dielectric properties at 100 kHz, and the microwave measurements, S11 reflection parameters, were achieved via interdigitated capacitor design with Au/Ag top electrodes. The parallel resistor-capacitor models were used to determine the microwave capacitance and Q factors, and the permittivity was calculated using a modified conformal-mapping partial-capacitance method using the dimension of the capacitors. Our results demonstrated that the low frequency and microwave frequency dielectric properties were strongly influenced by the film composition. Specifically, the Mg doping served to lower the dissipation factor, permittivity, and tunability of the BST based films at both frequencies. This work demonstrates that the BST based thin films possessed excellent microstructural, structural, and dielectric properties. The structure-process-property correlations of the pulsed laser deposited BST and acceptor doped BST-based thin films are discussed in detail.					
15. SUBJECT TERMS Ba <sub>1-x</sub> Sr <sub>x</sub> TiO <sub>3</sub> , thin films, tunable device					
16. SECURITY CLASSIFICATION OF:			17. LIMITATION OF ABSTRACT	18. NUMBER OF PAGES	19a. NAME OF RESPONSIBLE PERSON
a. REPORT UNCLASSIFIED	b. ABSTRACT UNCLASSIFIED	c. THIS PAGE UNCLASSIFIED			UL
					19b. TELEPHONE NUMBER (Include area code) 410-306-0748

---

## Contents

---

<b>List of Figures</b>	<b>iv</b>
<b>List of Tables</b>	<b>iv</b>
<b>1. Introduction</b>	<b>1</b>
<b>2. Experiments</b>	<b>1</b>
<b>3. Results and Discussion</b>	<b>3</b>
<b>4. Conclusions</b>	<b>5</b>
<b>5. References</b>	<b>6</b>
<b>Distribution List</b>	<b>7</b>

---

## List of Figures

---

Figure 1. Diagram of interdigitated capacitors (IDC) with microwave probe in contact. Finger length of the device is 80 $\mu\text{m}$ and finger width spacing is 6 $\mu\text{m}$ .....	2
Figure 2. X-ray diffraction of (a) BST and (b) BST-5 mole% doped MgO annealed at 750 $^{\circ}\text{C}$ . .....	3
Figure 3. Micrographs of the BST based film: (a) AFM plan view and (b) FESEM cross sectional. ....	4
Figure 4. The microwave dielectric properties as a function of frequency at 0 and 40 V bias. ....	5

---

## List of Tables

---

Table 1. Summary of dielectric and insulating properties of undoped and Mg doped $\text{Ba}_{1-x}\text{Sr}_x\text{TiO}_3$ thin films at frequency of 100 kHz.....	5
--	---

---

## 1. Introduction

---

In recent years, there has been a significant increase in the need for, and applications of, microwave circuit technologies. The progress in the communication application area has resulted in a demand for miniaturized components, which are a key factor for low power and integratable microwave devices (1–4). Ferroelectric films have attracted considerable attention for applications in computer memory elements, frequency-agile microwave components, pyroelectric sensors, and voltage tunable capacitors (3–8). For tunable device applications, the ferroelectric material should possess low dielectric loss, low leakage current, and high-voltage tunability (4). A promising candidate material is  $\text{Ba}_{1-x}\text{Sr}_x\text{TiO}_3$  (BST). BST is a continuous solid solution between barium titanate and strontium titanate over the entire range of concentration. The Curie temperature of  $\text{Ba}_{1-x}\text{Sr}_x\text{TiO}_3$  decreases linearly with increasing strontium titanate concentration. As a result, the transition temperature and, hence, the dielectric and optical properties of  $\text{Ba}_{1-x}\text{Sr}_x\text{TiO}_3$  can be tailored over a broad range to meet the requirements of various electronic device applications.  $\text{Ba}_{1-x}\text{Sr}_x\text{TiO}_3$ -MgO-based bulk and single-layer composite materials have shown excellent dielectric loss and dielectric tunability characteristics at X-band and K-band frequencies compared to those of pure BST bulk ceramics (7–11). However, a major drawback of these bulk ceramics for tunable devices, such as phase shifting elements, is the large drive voltages required for phase shifting (2). Thin films, with optimized dielectric and insulating material properties, are required to significantly lower the operating voltages. Such optimized thin films will also offer the additional advantages of a light weight, compactness, and intergratebility (2, 4, 6).

---

## 2. Experiments

---

The BST-based thin films were fabricated via the pulsed laser deposition (PLD) technique. Details of the PLD technique has been described elsewhere (4). High-density stoichiometric sintered ceramic targets of  $\text{Ba}_{(0.6)}\text{Sr}_{0.4}\text{TiO}_3$  and 5 mol% Mg-doped  $\text{Ba}_{(0.6)}\text{Sr}_{0.4}\text{TiO}_3$  were used to fabricate the thin films. Optimizing condition for PLD were investigated using four different sets of films. Each were deposited at different parameters condition then characterized by XRD in conjunction with residual stresses. Parameters condition, including changing in power density ( $\text{J}/\text{cm}^2$ ), partial oxygen pressure (mTorr), time of deposition (minutes), and substrates temperature ( $T_s$ ) were observed. Final films were grown on (100) MgO single crystal substrates with a substrate temperature of  $700\text{ }^\circ\text{C}$ . The films were deposited using a 248-wavelength Lambda Physik excimer laser with an energy density of  $2.5\text{ J}/\text{cm}^2$  and an oxygen pressure

of 70 mTorr. The nominal film thickness was 600 nm. Subsequent to deposition, the films were annealed at temperatures ranging from 550 to 1000 °C for 1 hr in oxygen. glancing angle x-ray diffraction (GAXRD), using a Bruker D5005 diffractometer with  $\text{CuK}\alpha$  radiation, was employed to assess film crystallinity. A Digital Instruments Dimension 3100 Atomic Force Microscope and a Hitachi S4500 field emission scanning electron microscope (FESEM) were utilized to assess film surface morphology and cross-sectional microstructure, respectively. The dielectric properties, at low frequency, were obtained in the metal-insulator-metal (MIM) capacitor configuration. The MIM capacitors were fabricated by sputtering 0.2-mm Pt dots separated by 0.5-mm spacing through a shadow mask over a  $1 \times 1 \text{ cm}^2$  area of the film surface. The dielectric properties were measured with an HP4194A impedance/gain-phase analyzer. The microwave frequency dielectric characterization, via interdigitated capacitors (IDCs), was obtained using standard photolithography and metal-liftoff patterning (4, 5). Subsequent to cleaning the samples in trichloroethane, acetone, and DI water, the interdigitated pattern was developed as a window in a three-layer resist consists of 1.5- $\mu\text{m}$  polymethylmethacrylate (PMMA), a 1000-Å layer of copper, and 1.5- $\mu\text{m}$  Microposit 1818 photoresist. The pattern was printed on the film by the screen-contact print method, and the 1818 resist was removed by UV flood exposure and developed using the 351 developers. A diagram of the IDC device design is shown in figure 1. A C+ program was used to control the internal bias and obtain the  $S_{11}$  parameters from the HP 8510 network analyzer. The devices were contacted by means of a signal-ground Picoprobe microwave probe. The initial pre-bias condition included a sweep bias from -40 to 40 V at 5-V/step functions. The dielectric constant was extracted using a modified conformal-mapping method using the dimension of the capacitors (6, 12).

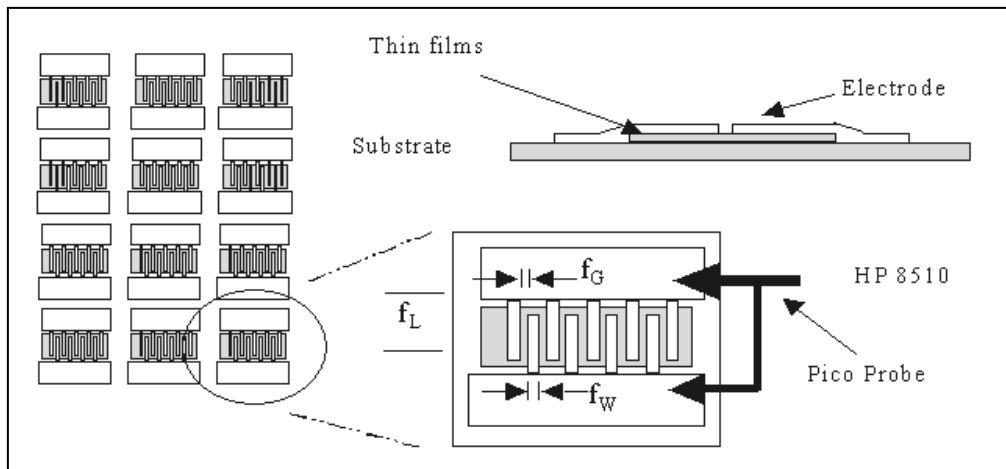


Figure 1. Diagram of IDCs with microwave probe in contact. Finger length of the device is 80  $\mu\text{m}$ , and finger width spacing is 6  $\mu\text{m}$ .

---

### 3. Results and Discussion

---

The as-deposited film ( $T_s$ - 700 °C), was amorphous, and post-deposition annealing was necessary to impart crystallinity. The post-deposition annealing of these films was carried out in an oxygen ambience at temperatures ranging from 550–1000 °C for 1 hr. At the annealing temperature of 600 °C, there were no diffraction peaks in the XRD patterns; however, at 650 °C and higher, the films became crystalline. Figure 2 displays the XRD pattern of the optimized 750 °C annealed-undoped and Mg-doped films. Both film compositions were polycrystalline with no evidence of secondary phase formation. The full width at half maximum (FWHM) of the (110) and (220) diffraction peaks for the Mg-doped BST was broader than that of the undoped BST suggesting a smaller grain size and for the doped film. An atomic force microscope (AFM) micrograph of the surface morphology, of the doped BST film is displayed in figure 3a. The AFM result demonstrates that the film is dense, crack and pinhole free. The average surface roughness was 9.3 and 6.3 nm for the undoped and doped films, respectively. These surface roughness values are acceptable for tunable device applications. It should be mentioned that the surface roughness can be lowered by lowering the laser fluence; however, this would be at the expense of decreasing the deposition rate ( $\phi$ ). Both film compositions exhibited a uniform grain size (78 nm for the undoped film and 64 nm for the Mg-doped film) after annealing at 750 °C. Figure 3b displays an FESEM cross-sectional image of the undoped BST film. The microstructure of the BST film exhibits columnar grain structure and possesses a smooth film/substrate interface.

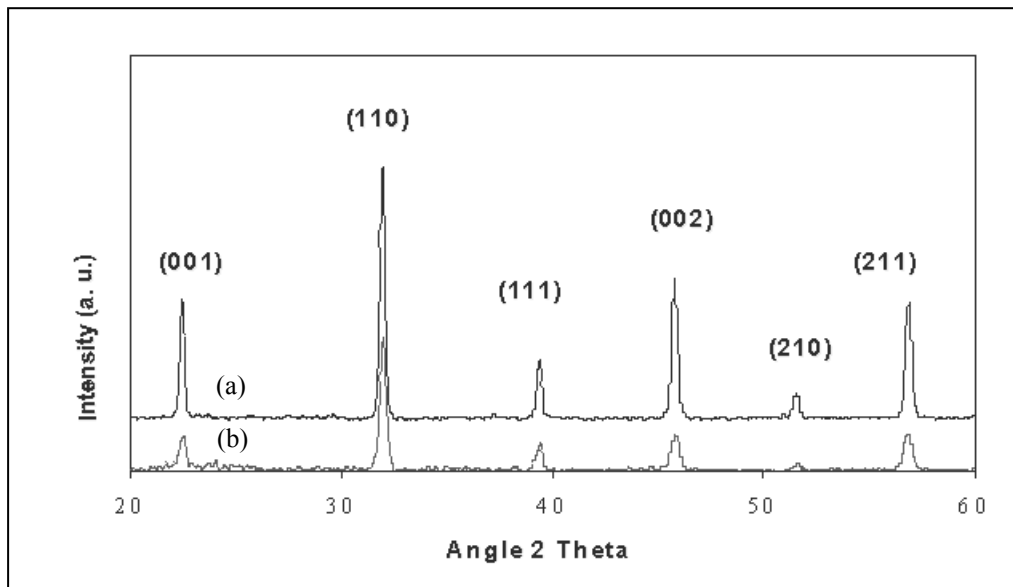


Figure 2. XRD of (a) BST and (b) BST-5 mole% doped MgO annealed at 750 °C.

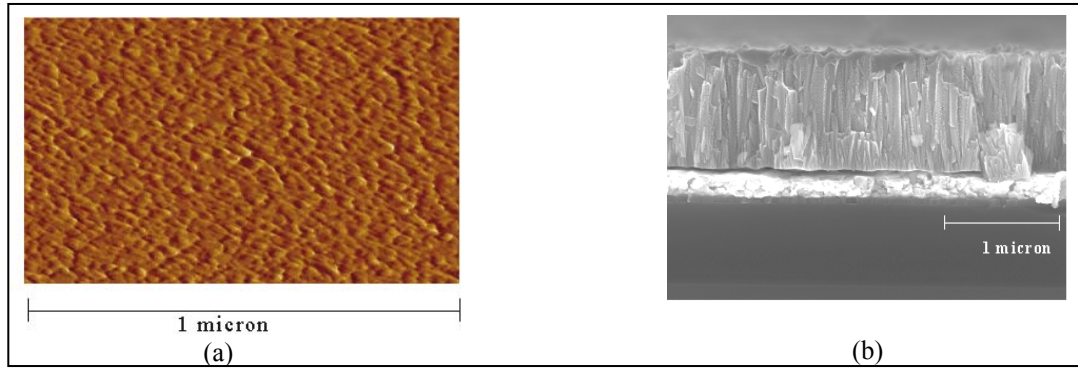


Figure 3. Micrographs of the BST based film: (a) AFM plan view and (b) FESEM cross sectional.

The dielectric properties were calculated using equations 1–4 (4).

$$\epsilon_r = (Ct_{\text{film}}) / A \epsilon_0, \quad (1)$$

$$\% \text{ Tu} = \Delta \epsilon_r / \epsilon_r(0) = [\epsilon_r(0) - \epsilon_r(\epsilon_{\text{max}})] / \epsilon_r(0), \quad (2)$$

$$C_{\text{total}} = f_l (N_{\text{finger}}, L_{\text{length}}, \epsilon_{\text{eff}}, C_{\text{per unit length}}), \quad (3)$$

and

$$\epsilon_{\text{eff}} = q_{\text{air}} \epsilon_{\text{air}} + q_{\text{film}} \epsilon_{\text{film}} + q_{\text{substrate}} \epsilon_{\text{substrate}}. \quad (4)$$

At low frequency (100 kHz), the film's dielectric properties were measured in terms of the capacitance  $C_p$  (calculated  $\epsilon_r$ ) and the loss tangent ( $\tan \delta$ ). A small alternate current (ac) signal of 10-mV amplitude from the HP 4192A impedance analyzer was applied to the MIM thin film capacitors. The permittivity and dielectric tunability were calculated using equations 1 and 2. The tunability was found to increase with increase of the applied electric field, for both film compositions.

At 200 kV/cm, the tunability was 50% for the undoped film and 19% for the doped film. The tunability for the undoped BST achieved a maximum value of 68% at 400 kV/cm. The tunability of a BST-based film can be elevated by lowering the Ba/Sr ratio; however, the resultant highly tunable compositions also exhibit higher dielectric loss (5). The dielectric properties of the undoped and doped BST films are displayed in table 1. At 100 kHz, the dielectric constant and dissipation factor of undoped and doped BST were 443.44/0.062 and 303.12/0.051, respectively. These results suggest a 25% reduction in permittivity and dielectric loss as a result of acceptor doping. The microwave dielectric properties are displayed in figure 4. The device measurement test structure, IDC, was fabricated on the 0.6- $\mu\text{m}$ -thick BST and BST-5% MgO-doped films deposited on MgO substrates. The equivalent of parallel combination of a resistor and capacitor was used for the calculation. At 40 V, the device showed a capacitance change from 3.4 to 2.6 pF, while device Q varied from 30 to 52. The change in capacitance translated to a dielectric

tunability of 28% with an average Q ( $Q = 1/\tan \delta$ ) of 40 ( $\tan \delta = 0.20$ ) at 10 GHz. The conformal mapping technique was used to extract the values of  $\epsilon_r$  and  $\tan \delta$  (12). The

Table 1. Summary of dielectric and insulating properties of undoped and Mg-doped  $\text{Ba}_{1-x}\text{Sr}_x\text{TiO}_3$  thin films at a frequency of 100 kHz.

Mg (mol%)	$\epsilon_r$	$\tan(\delta)$	Tunability (at 200kV/cm) (%)	$I_L$ (A) (at 200kV/cm)
0	443.44	0.062	50.1	$0.22 \times 10^{-11}$
5	303.12	0.051	18.9	$0.15 \times 10^{-11}$

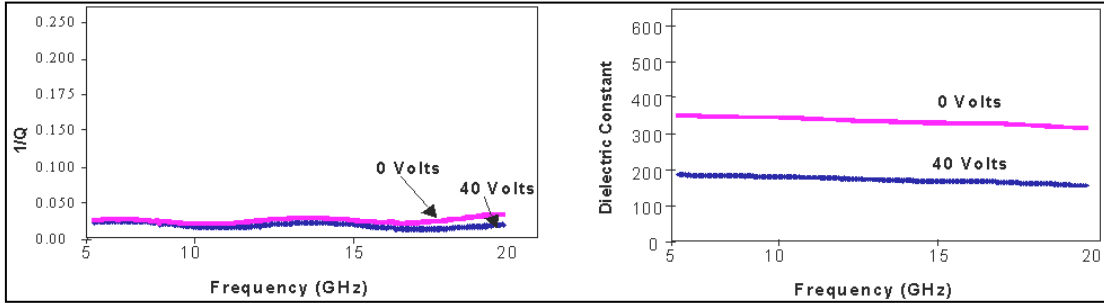


Figure 4. The microwave dielectric properties as a function of frequency at 0- and 40-V bias.

dielectric constant and loss at the sweep frequency, ranging from 5–20 GHz, were 345.0 and 0.025, respectively. It is suggested by Kirchoefer et al. (5) that the fractional change in relative permittivity with bias is larger than the fractional change of the device capacitance because the substrate and air contribute to the device capacitance and are in parallel with the ferroelectrics capacitance. Similar conditions are true for  $\tan \delta$  of the film, which is larger than the reciprocal of the device Q. In general, the low and microwave frequency dielectric properties of both film compositions appear desirable for tunable device applications.

---

## 4. Conclusions

---

Undoped and Mg-doped paraelectric thin films deposited by PLD have been shown to produce high-quality films on (100) MgO substrates. The films were well crystallized after post-deposition, annealing at 750 °C for 1 hr. The undoped and doped films possessed low dielectric loss and good tunability at both low (100 kHz) and microwave (0.5–20 GHz) frequency. The improved dielectric properties of pure and Mg doped BST thin films suggest their suitability for tunable device applications. Future work will focus on identifying the key elements responsible for improved dielectric tuning and low dielectric loss in these films.

---

## 5. References

---

1. Joshi, P. C.; Desu, S. B. *Applied Physics Letters* **1998**, *73*, 1080.
2. Cole, M. W; Joshi, P. C.; Ervin, M. H.; Wood, M. C.; Pfeffer, R. L. *Thin Solid Films* **2000**, *374*, 34.
3. Cukauskas, E. J.; Kirchoefer, S. W.; DeSisto, W. J.; Pond, J. M. *Applied Physics Letters* **1999**, *74*, 4034.
4. Chang, W.; Horwitz, J. S.; Carter, A. C.; Kirchoefer, S. W.; Gilmore, C. M.; Chrisey, D. B. *Applied Physics Letters* **1999**, *74* (7) 1003.
5. Kirchoefer, S. W.; Pond, J. ; Carter, A. C.; Chang, W.; Agarwal, K. K.; Horwitz, J. S.; Chrisey, D. B. *Microwave and Optical Technical Letters* **1998**, *18*, 3.
6. Cole, M. W.; Joshi, P. C.; Ervin, M. H. *Journal of Applied Physics* **2001**, *89*, (11).
7. Joshi, P. C.; Ryu, S. O.; Zhang, X.; Desu, S. B. *Applied Physics Letters* **1997**, *70*, 1080.
8. Joshi, P. C.; Cole, M. W. *Applied Physics Letters* **2001**, *77*, 289.
9. Sengupta, L. C.; Ngo, E.; Synowcznski, J. *Integrated Ferroelectrics* **1997**, *17*, 287.
10. Babbit, R. W.; Kosica, T. E.; Drach, W. E. *Microwave Journal* **1992**, *35*, 63.
11. Geyer, R. G.; Grosvenor, J. H.; Synowsynski, J. *Journal of Ceramic Transactions* **1999**, *106*, 36.
12. Gevorgain, S. S.; Martinsson, T.; Linner, P. I. J.; Kollberg, E. L. *IEEE Transactions on Microwave Theory Technology* **1996**, *44*, 896.

NO. OF  
COPIES ORGANIZATION

1 DEFENSE TECHNICAL  
(PDF INFORMATION CTR  
ONLY) DTIC OCA  
8725 JOHN J KINGMAN RD  
STE 0944  
FT BELVOIR VA 22060-6218

1 COMMANDING GENERAL  
US ARMY MATERIEL CMD  
AMCRDA TF  
5001 EISENHOWER AVE  
ALEXANDRIA VA 22333-0001

1 INST FOR ADVNCD TCHNLGY  
THE UNIV OF TEXAS  
AT AUSTIN  
3925 W BRAKER LN STE 400  
AUSTIN TX 78759-5316

1 US MILITARY ACADEMY  
MATH SCI CTR EXCELLENCE  
MADN MATH  
THAYER HALL  
WEST POINT NY 10996-1786

1 DIRECTOR  
US ARMY RESEARCH LAB  
AMSRD ARL CS IS R  
2800 POWDER MILL RD  
ADELPHI MD 20783-1197

3 DIRECTOR  
US ARMY RESEARCH LAB  
AMSRD ARL CI OK TL  
2800 POWDER MILL RD  
ADELPHI MD 20783-1197

3 DIRECTOR  
US ARMY RESEARCH LAB  
AMSRD ARL CS IS T  
2800 POWDER MILL RD  
ADELPHI MD 20783-1197

NO. OF  
COPIES ORGANIZATION

ABERDEEN PROVING GROUND

1 DIR USARL  
AMSRD ARL CI OK TP (BLDG 4600)

NO. OF  
COPIES ORGANIZATION

ABERDEEN PROVING GROUND

5 DIR USARL  
AMSRD ARL WM MA  
E NGO